Generation of Millimeter Waves by Photomixing at 1.55 μm Using InGaAs–InAlAs–InP Velocity-Matched Distributed Photodetectors

T. Chau, N. Kaneda, T. Jung, A. Rollinger, S. Mathai, Y. Qian, T. Itoh, M. C. Wu, W. P. Shillue, and J. M. Payne

***Abstract*—Millimeter-wave generation by photomixing at 1.55 μm in long-wavelength velocity-matched distributed photodetector (VMDP) is experimentally demonstrated. The VMDP exhibits a dc responsivity of 0.25 A/W, a breakdown voltage of 7–9 V, and up to 15-mA dc photocurrent without damage. Millimeter-wave output powers of −21 dBm at 75 GHz and −24 dBm at 95 GHz were measured.**

***Index Terms*—Distributed photodetector, high-speed, InAlAs, InGaAs, InP, millimeter-wave generation, MSM photodetector, optical heterodyne, photomixer.**

I. Introduction

MILLIMETER- and submillimeter-wave generation by photomixing in an ultrafast photodetector is a promising technique for radio astronomy [1]. In the last few years, remarkable progress has been made in the development of high-speed, high-power photodetectors, as reviewed in [2], [3], and ref. in [4]. In terms of applications, the high-speed photodetectors can be divided into four general categories: 1) high-speed digital communication systems; 2) RF photonic systems; 3) ultrafast optoelectronic sampling; and 4) optoelectronic generation of millimeter waves and submillimeter waves. Each application has different requirements [4]. For millimeter-wave and THz generation by optical heterodyning, the photodiodes are often referred to as photomixers. The frequencies of interest for photomixers ranges from 100 GHz to several terahertz. The most important parameter for photomixers is the amount of power that can be generated in a given bandwidth without damaging the photomixer. LT–GaAs photomixers with 1 μW of power at 600 GHz and somewhat lower power at 1 THz have been reported [5], [6]. The first successful use of a LT–GaAs photomixer as a source for the local oscillator in a 630-GHz radio astronomy receiver was reported in [7].

For distribution of local oscillator signals in a radio astronomy antenna array, long-wavelength photomixers operating at 1.55 μm are preferred due to low fiber loss, availability of high-power erbium-doped fiber amplifiers (EDFAs), tunable lasers, and other fiber components, thanks to the rapid advances of optical fiber communications technology. To date, there have been very few reports on millimeter-wave photomixers at 1.55 μm. Saturation output of 12 dBm at 60 GHz was reported by mixing optical pulses from a mode-locked laser diode in a Uni-Traveling-Carrier Photodiode (UTC-PD) [8]. A continuous wave (*CW*) power of −24 dBm at 60 GHz was reported using traveling wave photodetectors [9]. Recently, we reported a W-band photomixer with −23 dBm *CW* power at 95 GHz [4]. In this letter, we will discuss the fabrication and experimental results of the W-band velocity-matched distributed photodetectors (VMDP).

Manuscript received January 26, 2000; revised May 1, 2000. This work was supported by ONR MURI on RF Photonics, NRAO, and DARPA THz program.

T. Chau, N. Kaneda, T. Jung, A. Rollinger, S. Mathai, Y. Qian, T. Itoh, and M. C. Wu are with the University of California, Electrical Engineering Department, Los Angeles, CA 90095-1594 USA (e-mail: tai@icsl.ucla.edu).

W. P. Shillue and J. M. Payne are with the National Radio Astronomy Observatory, Tuscon, AZ 85721-0655 USA.

Publisher Item Identifier S 1041-1135(00)06270-4.

II. Device Structure and Fabrication

The principle of VMDP has been discussed in detail in [2]. Fig. 1 shows the schematic of VMDP. It consists of a linear array of photodetectors serially distributed over a transparent optical waveguide. Light is coupled evanescently from the waveguide to the photodetectors. Photocurrent is generated by each photodiode and collected by a 50-Ω coplanar strip (CPS) microwave transmission line. The CPS signal is designed to propagate at the same velocity as light in the optical waveguide so that the photocurrent from each diode adds in phase. This velocity matching is achieved by periodic capacitive loading of the CPS by the photodiodes. The active photodiode, optical waveguide, and microwave transmission line are independently designed for optimized performance.

The wafer was grown by metalorganic chemical vapor deposition (MOCVD) technique. Fig. 2 shows the schematic cross section of the wafer epitaxial layers. All layers are intrinsic and lattice matched to InP. The bottom four layers are designed to be transparent to light at both 1.3- and 1.55-μm wavelengths, and form the passive optical waveguide with 0.5-μm core. The top three layers form the active photodiode. The active photodiode consists of a 0.15-μm $In_{0.53}Ga_{0.47}As$ absorption layer, followed by a layer with a linearly graded bandgap and a thin $In_{0.52}Al_{0.48}As$ Schottky barrier enhancement layer to reduce leakage current. The linearly graded bandgap layer was used to smooth out the bandgap discontinuity between InAlAs and InGaAs, and reduce the carrier trapping effect in InAlAs–InGaAs photodiodes [10].

The fabrication process for VMDP is as follows: 1) 200-Å Ti/1000 Å Au metal markers for alignment of subsequent masks and E-beam writing are defined by standard liftoff technique; 2) active mesas with 14 × 16μm^2 areas are defined by wet etching down to the *Upper Cladding II Layer*. The etching is

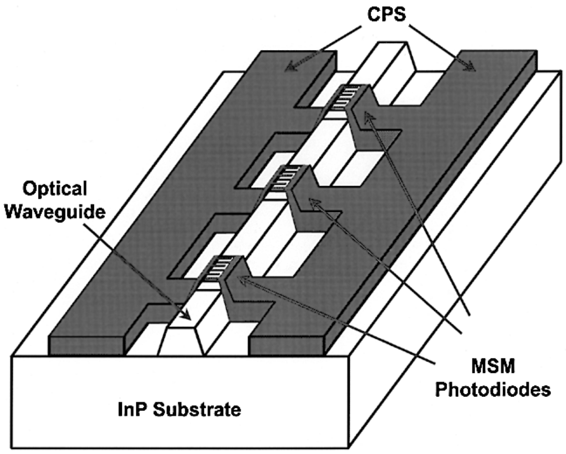

Fig. 1. Schematic structure of W-band VMDP.

done in two separate steps. First, the wafer is etched nonselectively midway into the InGaAs absorption layer by using a 1-$H_3PO_4 : 8\ H_2O_2 : 60\ H_20$ solution [11]. This etchant is nonselective for InGaAs–InAlAs–InAlGaAs, with an effective etch rate of 57 Å/s. Selective etchant with 1 $C_6H_8O_7 : 2\ H_2O_2$ was used to completely remove the remaining InGaAs active layer without etching into the InAlAs *Upper Cladding II Layer* [12]. The effective etch rate was 16 Å/s for InGaAs, and somewhat lower than 1 Å/s for InAlAs; 3) next, submicrometer metal-semiconductor-metal (MSM) fingers with metal thickness of 100-Å Ti/100 Å Pt/500 Å Au are patterned on top of the mesas by E-beam writing followed by standard liftoff. The finger width is 200 nm, and spacing between the fingers is 200 nm. 4) Multimode nonabsorbing optical ridge waveguide with 1.1-μm ridge height, 16-μm-wide is patterned by nonselective wet etching down to the InP substrate to connect all the active diodes defined by 2) and 3). 5) Finally, contact pads to the MSM fingers and the CPS microwave transmission line with metal thickness of 200-Å Ti/300 Å Pt/3500 Å are patterned. The CPS has a metal line width of 100 μm and a gap of 30 μm. The finished wafer is then lapped down to 75 μm, cleaved and mounted on copper heat sink for testing.

III. Experimental Results

The device under test (DUT) consists of 4 MSM photodiodes, each with 14-μm length and 148-μm spacing between diodes. The VMDP exhibits very high breakdown voltage, from 7 to 9 V, which corresponds to 3.5–4.5 $\times$ 10^5V/cm. DC responsivity greater than 0.25 A/W at 5-V bias has been measured. Fig. 3 shows the dc photocurrent versus input optical power for DUT at 5-V bias. The frequency response of the VMDP is characterized by the optical heterodyne method [13], [14]. Schematic of the experimental setup is shown in Fig. 4. Light from two external cavity tunable lasers at 1.55 μm is combined by a 3-dB coupler. The combined signals are amplified by a high-power EDFA with 30-dBm saturation power. A 1-nm optical band-pass filter was used to reduced the amplified spontaneous emission (ASE) noise from the EDFA. A dual purpose in-line optical power attenuator/power monitor was used to control the input optical power to the DUT. The signal is coupled to the VMDP through a fiber pickup head. A commercial probe with a built-in Bias-T was used to probe the device, converting CPS to W-Band (75–100 GHz) waveguide. The dc port of the Bias-T is connected to a commercial power supply with dc photocurrent monitoring. The millimeter-wave output signal was delivered to a calibrated W-band power sensor and measured by a power meter. The calibrated frequency response of the VMDP is shown in Fig. 5. This response includes both VMDP and

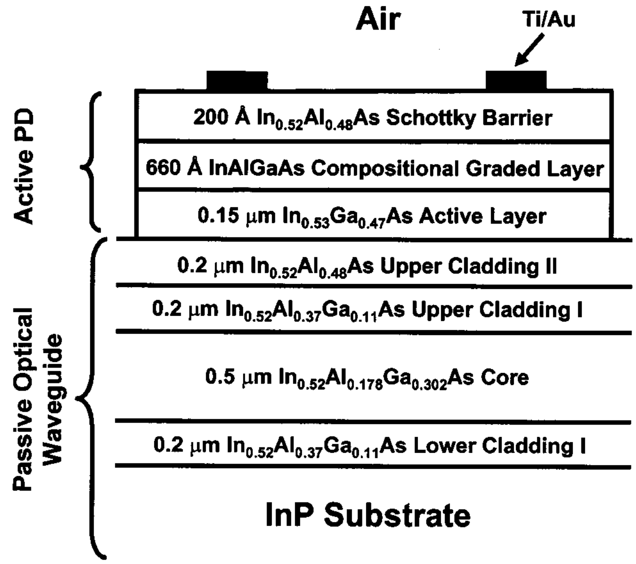

Fig. 2. Cross section of the wafer epitaxial layers after mesa etching.

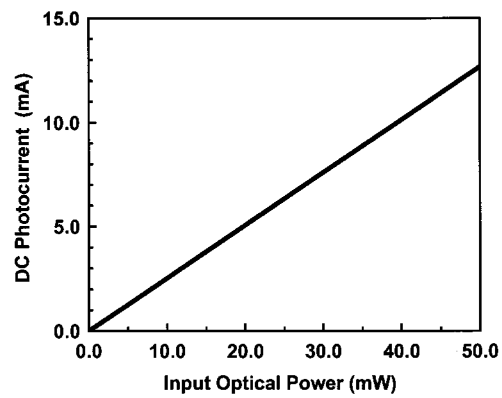

Fig. 3. DC photocurrent versus input optical power for W-band VMDP at 5-V bias.

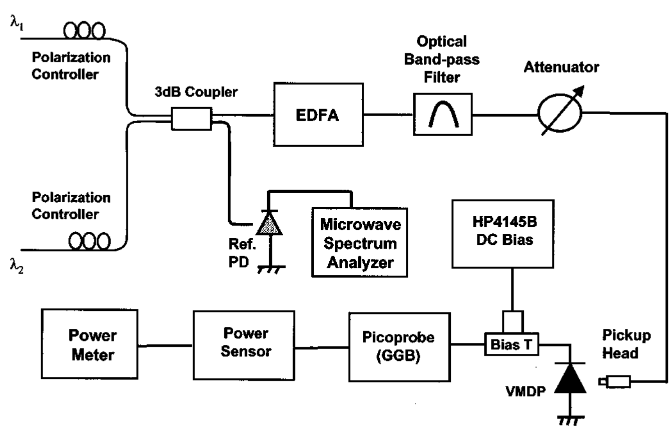

Fig. 4. Schematic of optical heterodyne setup.

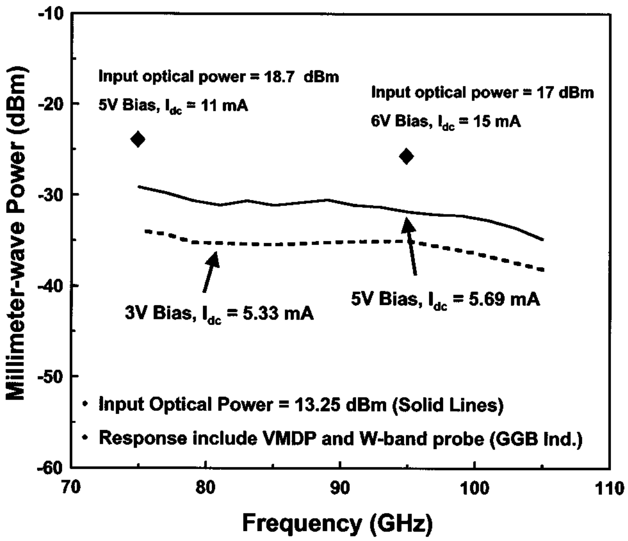

Fig. 5. VMDP response versus bias voltage at W-band. Maximum output power at 75 and 95 GHz are also shown.

W-band probe. The device is bias dependent, with higher output power at higher dc bias. The solid lines show the broadband response of the device at 3- and 5–V dc bias, with the same input optical power of 13.25 dBm. Further increase of the bias voltage yields no further increase of the output power. The frequency band was scanned by tuning the wavelength of one of the external cavity lasers. An appropriate calibration factor for the power sensor was used at each frequency. The signal rolloff was small across the entire W-band. To measure the maximum output power from the device, the dc bias and the difference frequency from the input lasers were fixed, and input optical power was adjusted using the attenuator. Maximum output signals of −23 dBm at 75 GHz, and −26 dBm at 95 GHz were measured. These power levels were measured over a period of minutes, long enough to reach thermal equilibrium with continuous-wave input, indicating a viable long-term operating level. Further increase of the optical input level resulted in damage to the device. Taking into account the W-band probe, with a nominal insertion loss of 2 dB from manufacturer's data, the VMDP maximum output signals are −21 dBm at 75 GHz and −24 dBm at 95 GHz.

IV. Conclusion

We have experimentally demonstrated millimeter-wave generation by photomixing at 1.55 μm using high-speed high-power VMDP. The device can sustain high photocurrent, up to 15 mA without damage. This indicates the potential of a much higher millimeter-wave output power if all the current were being converted at high frequency. Millimeter-wave output power of −21 dBm at 75 GHz and −24 dBm at 95 GHz were measured. To our knowledge, this is the highest CW millimeter-wave power generated by photomixing at 1.55 μm at these frequencies. Higher power can be achieved by improving design for better conversion of photocurrent to millimeter-wave output power, adding more photodiodes per VMDP, and employing narrow band microwave design for higher efficiency at the desired bandwidth.

Acknowledgment

The authors would like to thank R. Muller and P. Maker at JPL for help with E-beam writing.

References

[1] J. Payne, B. Shillue, and A. Vaccari, "Photonic techniques for use on the atacama large millimeter array," presented at the IEEE MWP'99, Melbourne, Australia, Nov. 17–19, 1999.

[2] L. Y. Lin, M. C. Wu, T. Itoh, T. A. Vang, R. E. Muller, D. L. Sivco, and A. Y. Cho, "High-power high-speed photodetectors. Design, analysis, and experimental demonstration," *IEEE Trans. Microwave Theory Tech.*, vol. 45, pp. 1320–1331, Aug. 1997.

[3] K. Kato, "Ultrawide-band, high-frequency photodetectors," *IEEE Trans. Microwave Theory Tech.*, vol. 47, no. 7, pp. 1265–1281, 1999.

[4] T. Chau, N. Kaneda, T. Jung, A. Rollinger, S. Mathai, Y. Qian, T. Itoh, M. C. Wu, B. Shillue, J. Payne, and D. Emerson, "High-speed velocity-matched distributed photodetectors," presented at the IEEE LEOS'99 Annu. Meeting, San Francisco, CA, Nov. 8–11, 1999.

[5] E. R. Brown, K. A. McIntosh, K. B. Nichols, and C. L. Dennis, "Photomixing up to 3.8 THz in low-temperature-grown GaAs," *Appl. Phys. Lett.*, vol. 66, pp. 285–287, 1995.

[6] S. Matsuura, G. A. Blake, R. A. Wyss, J. C. Pearson, C. Kadow, A. W. Jackson, and A. C. Gossard, "A traveling-wave THz photomixer based on angle-tuned phase matching," *Appl. Phys. Lett.*, vol. 74, pp. 2872–2874, 1999.

[7] S. Verghese, E. K. Duerr, K. A. McIntosh, S. M. Duffy, S. D. Calawa, C.-Y. E. Tong, R. Kimberk, and R. Blundell, "A photomixer local oscillator for a 630-GHz heterodyne receiver," *IEEE Microwave Guide Wave Lett.*, vol. 9, pp. 245–247, June 1999.

[8] T. Nagatsuma, N. Sahri, M. Yaita, T. Ishibashi, N. Shimizu, and K. Sato, "All optoelectronic generation and detection of millimeter-wave signals," presented at the IEEE MWP'98, Princeton, NJ, Oct. 12–14, 1998.

[9] M. Alles, U. Auer, F.-J. Tegude, and D. Jäger, "Distributed velocity-matched 1.55 mm InP travelling-wave photodetector for generation of high-millimeterwave signal power," in *IEEE MTT-S Dig*, 1998, pp. 1233–1236.

[10] D. H. Lee, S. S. Li, N. J. Sauer, and T. Y. Chang, "High-quality $In_{0.53}Ga_{0.47}As$ Schottky diode formed by graded superlattice of $In_{0.53}Ga_{0.47}As$-$In_{0.52}Al_{0.48}As$," *Appl. Phys. Lett.*, vol. 54, no. 19, pp. 1863–1865, 1989.

[11] A. Stano, "Chemical etching characteristics of InGaAs-InP and InAlAs-InP heterostructures," *J. Electrochem. Soc.*, vol. 134, no. 2, pp. 448–452, 1987.

[12] G. C. DeSalvo, W. F. Tseng, and J. Comas, "Etch rates and selectivities of citric acid/hydrogen peroxide on GaAs, $Al_{0.3}Ga_{0.7}As$, $In_{0.2}Ga_{0.8}As$, $In_{0.53}Ga_{0.47}As$, $In_{0.52}Al_{0.48}As$, and InP," *J. Electrochem. Soc.*, vol. 139, no. 3, pp. 831–835, 1992.

[13] T. Hawkins II, M. D. Jones, S. H. Pepper, and J. H. Goll, "Comparison of fast photodetector response measurement by optical heterodyne and pulse response techniques," *J. Lightwave Technol.*, vol. 9, pp. 1289–1294, 1991.

[14] P. D. Hale, D. A. Humphreys, and A. D. Gifford, "Photodetector frequency response measurements at NIST, U.S.A., and NPL, U.K.: Preliminary results of a standards laboratory comparison," in *Proc. SPIE*, vol. 2149, 1994, pp. 345–356.